Motion Compensation System for a free floating Surface Effect Ship ⋆

Øyvind F. Auestad *,** **Jan T. Gravdahl** *
Asgeir J. Sørensen *** **Trygve H. Espeland** **

* *Dept. of Eng. Cybernetics, O. S. Bragstads plass D, NTNU, N-7491 Trondheim, Norway; e-mail: oyvind.auestad@itk.ntnu.no*
** *Umoe Mandal AS Gismerøyveien 205, N-4515 Mandal, Norway*
*** *Centre for Autonomous Marine Operations (AMOS), Dept. of Marine Technology, Otto Nielsens vei 10, NTNU, N-7491, Trondheim, Norway*

Abstract: This paper deals with vertical motion compensation, or motion damping, on a free-floating Surface Effect Ship (SES) at zero speed. The Motion Compensation System (MCS) works by varying the air cushion pressure of a Surface Effect Ship (SES) to minimize vertical motion due to sea waves. We present a control system which guarantees Global Exponential Stability for the closed-loop state space system and ultimately boundedness for the perturbed system. A study of the performance of the control system is demonstrated through model-test results of a 3 meter long SES.

Keywords: Marine systems, Lyapunov stability, automatic control (closed-loop).

1. INTRODUCTION

1.1 The SES Concept

Surface Effect Ships are known to offer high speed and excellent sea keeping performance in high sea states compared to conventional catamarans. The SES rides on an air cushion which is enclosed by to two catamaran side hulls and flexible rubber seals in the bow and stern end, see fig. 1. A great advantage of SES over a hovercraft, or an Air Cushion Vehicle (ACV), is that the rigid side hulls permit the use of water jet propulsion which enables a high and efficient transit speed. The air cushion is pressurized using a set of lift fans that blow air into the air cushion. The cushion lifts the vessel vertically, and the pressurized air can carry the majority of the vessel weight.

Fig. 1. SES hull, bag and bow seal (photo: Umoe Mandal)

The pressure is indirectly controlled by varying the leakage area A_L out of the air cushion using ventilation valves. By controlling the air flow actuators, a SES at zero speed, can alter its lift force in counter-phase with the sea waves. The controlled air cushion pressure acts as a compensator to the motion set up by sea wave propagations. Hence the control system is called a compensation system.

A comprehensive study on the SES is presented by Butler (1985). More recent literature involves the T-Craft and (Doctors, 2012) which focus on hydrodynamics. Also, Basturk and Krstic (2013) reduces ramp motions between a large, medium-speed, roll-on/roll-off (LMSR) vessel and a SES by controlling the air cushion pressure which resembles the problem formulation of this article.

Modelling and control of the air cushion during transit are covered by Kaplan and Davies (1974) and Sørensen and Egeland (1995).

This paper presents stability analysis and performance properties of the Motion Compensation System (MCS) using experimental model-test results. This document complements Auestad et al. (2013b) which presents mathematical modelling and development of a comprehensive simulator toolbox that captures the dynamics of a SES. Also, simulation of the MCS is presented.

1.2 Motivation

The craft of interest is the Offshore Wind Farm Service Vessel, the UM Wave Craft.

Operation and Maintenance (O&M) costs constitute a sizeable share of an offshore wind farm, in fact, 20% to 30% of the total levelized cost of energy (Musial and Ram, 2010). Decreasing O&M costs includes minimization of maintenance time requirements and maximization of access feasibility (EWEA, 2013).

The Wave Craft, which is a Umoe Mandal high speed craft with speed capability of up to 45 knots is currently

⋆ A special thanks is handed out to Umoe Mandal (UM) for sharing information and being helpful

Fig. 2. The UM Wave Craft (photo: Umoe Mandal)

under construction. It is a craft with very narrow side hulls. This means that only a small area is exposed to hydrodynamic disturbances which will reduce vertical bow motion. In addition, the craft automatically controls the pressure inside the air cushion to further maximize access feasibility. By utilizing active control of the air cushion pressure to stabilize vertical motion, the vessel is able to dock with offshore wind turbines in higher sea states than possible today.

This docking scheme consists of two phases. In this paper, *Phase One* is studied.

• *Phase One:* Deals with a free-floating SES that uses automatic control to alter the air cushion pressure in order to compensate for motions induced by wave forces. The pressure is controlled in such a way that the vertical motion of the bow tip is minimized. In section 4 (Model Test Results), this is denoted "Bow Pos.". Phase one prepares the vessel for phase two.

• *Phase Two:* In this phase, the captain will allocate sufficient thrust force from the water jets, which will result in a mechanical friction force that will hinge the craft bow rubber fender to the turbine. At this point, the cushion pressure is actively controlled so that the friction force is larger than the excitations force. A paper describing the second phase will be published at a later stage.

1.3 Model Testing

The proposed control system was tested in waves using a 3 meter long model of the Wave Craft. The hull, lift fans, seals and ventilation valves are correctly scaled and modelled to fit the designed full-scale properties. The main dimensions of the craft are given in app. B and the scaling factor is 8.

The paper is organized as follows. Section 2 is about modelling the most important dynamics used for the control system design discussed in section 2.2 and the stability analysis which is discussed in section 3. Section 4 presents experimental model test results and we conclude our work in section 5.

2. CONTROL PLANT MODEL

The mathematical model presented is used for stability analysis. For a more detailed process plant model, suitable for craft simulation, see Auestad et al. (2013b).

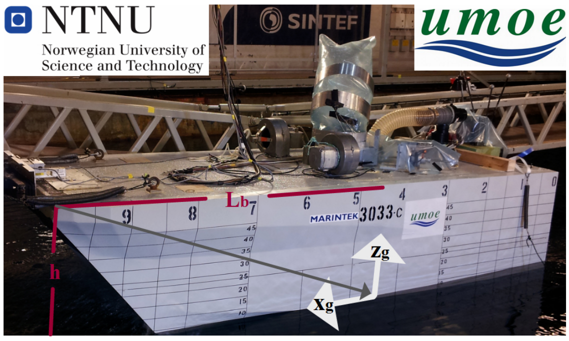

Fig. 3. The picture shows the 3 meter long model test craft of the UM Wave Craft

Equations of motion and cushion pressure dynamics for a SES were first presented by Kaplan and Davies (1974). The equations consider three coupled degrees of freedom, uniform pressure, heave and pitch. A decoupled version of pressure, heave and pitch was presented in Sørensen and Egeland (1995) which forms the basis of this work.

A body-fixed coordinate system is defined according to the right hand rule with the x_g, y_g and z_g-axes oriented positive forwards, to the port and upwards respectively. The origin is located on the mean water plane, under the center of gravity, as illustrated in figure 3. All equations of motion are formulated in this frame. One thing differs from the control plant model presented in Sørensen and Egeland (1995), but is defined in the process plant model in Sørensen (1993):

Assumption 1. A coupling exist between cushion pressure, and pitch velocity.

This assumption is justified by the large variations of cushion pressure that occurs during MCS. The point of attack for the air cushion pressure does not coincide with the hydrodynamic point of attack, which is our origin. The longitudinal distance between these points is denoted x_{cp} and is considered to be too large to neglect.

Translation along the z_g-axis is called heave and denoted η_3, while the rotation angle around the y_g-axis is called pitch and denoted η_5. The remaining degrees of freedom, which are not relevant in this article, includes η_i, where $i = 1, 2, 4$ and 6 which respectively denotes surge, sway, roll and yaw.

The SES dynamics in the vertical plane are modelled as a mass-spring-damper system with sea wave excitation forces and air cushion volume pumping as disturbances.

The following equations (1) - 10) are based on Sørensen (1993). The total pressure inside the air cushion is described as

$$P_c(t) = P_a + P_u(t) \tag{1}$$

where P_a is the atmospheric pressure, and $P_u(t)$ is uniform cushion excess pressure.

The lift fans are assumed to run at constant speed supplying the air cushion with an air inflow $Q_{in}(t)$ which is given according to a linearised fan characteristic. The cushion air outflow $Q_{out}(t)$ varies proportionally to the ventilation valve leakage area A_L defined as

$$A_L(t) = A_{L,Bias} + \Delta A_L(t), \tag{2}$$

where $A_{L,Bias}$ is a certain constant valve opening, allowing controlled area variations (ΔA_L) in both directions. The vessel will reach it's equilibrium state when $\Delta A_L = 0$ and no sea waves are present. In this case, the cushion excess pressure reaches its equilibrium pressure P_0, hence $P_u(t) = P_0$. The system will be linearised about this point.

For modelling purposes, a non-dimensional uniform pressure variation $\mu_u(t)$ is defined according to

$$\mu_u(t) = \frac{P_u(t) - P_0}{P_0} \tag{3}$$

The equations of motion in heave and pitch are written as

$$(m+A_{33})\,\ddot{\eta}_3(t)+B_{33}\,\dot{\eta}_3(t)+C_{33}\,\eta_3(t)-A_c\,P_0\,\mu_u(t) = F_3^e(t), \tag{4}$$

$$(I_{55}+A_{55})\ddot{\eta}_5(t)+B_{55}\dot{\eta}_5(t)+C_{55}\eta_5(t)+A_c\,P_0\,x_{cp}\,\mu_u(t) = F_5^e(t), \tag{5}$$

where m is vessel mass, and I_{55} is the moment of inertia about the body fixed y-axis. A_c is equilibrium air cushion surface-area. Let j = 3,5 respectively denote heave and pitch motions. Then, A_{jj} is hydrodynamic added-mass coefficient, B_{jj} is the water wave radiation damping coefficient and C_{jj} is a hydrostatic coefficient due to buoyancy. F_j^e is the hydrodynamic excitation force acting on the sidehulls.

The hydrodynamic excitation forces in heave and pitch can be expressed as:

$$F_3^e(t) = 2\zeta_a e^{-\kappa\,d}\frac{sin\frac{\kappa\,L}{2}}{\frac{\kappa\,L}{2}}\left(C_{33}-\omega_0^2 A_{33}\right)sin\,\omega_0 t, \tag{6}$$

$$F_5^e(t) = 2\zeta_a e^{-\kappa\,d}\Bigg[\left(\frac{1}{\kappa}cos\frac{\kappa\,L}{2} - \frac{2}{\kappa^2\,L}sin\frac{\kappa\,L}{2}\right)\left(C_{33}-\omega_0^2 A_{33}\right)\Bigg]cos\,\omega_0 t \tag{7}$$

where $\kappa = 2\pi/\lambda$. ζ_a, λ and ω_0 are respectively sea wave elevation amplitude, length and frequency, L is air cushion length, d is the draft of side hulls.

The uniform cushion pressure equation is expressed as:

$$K_1\,\dot{\mu}_u(t)+K_3\,\mu_u(t)+\rho_{c0}\,A_c\,\dot{\eta}_3(t)-\rho_{c0}A_c x_{cp}\dot{\eta}_4(t) = K_2\;\Delta A_L(t)+\rho_{c0}\,\dot{V}_0(t), \tag{8}$$

where:

$$\begin{aligned} K_1 &= \frac{\rho_{c0}\,h_0\,A_c}{\gamma\left(1+\frac{P_a}{P_0}\right)},\\ K_2 &= \rho_{c0}\,c_n\sqrt{\frac{2P_0}{\rho_a}},\\ K_3 &= \frac{\rho_{c0}}{2}\left(Q_0 - 2\,P_0\,q\frac{\partial Q_{in}}{\partial P}|_0\right), \end{aligned} \tag{9}$$

where h_0, ρ_{c0} respectively denote the height from the waterline to the wet-deck and air density, both at equilibrium cushion pressure. ρ_{c0} can be approximated to ρ_a, air density at ambient conditions. Q_0 is the equilibrium air flow rate, $\frac{\partial Q_{in}}{\partial P}|_0$ is the lift fan characteristic slope at equilibrium point, q is the total number of (identical) lift fans, $\dot{V}_0(t)$ is the rate of wave volume pumping for the dynamic pressure. Volume pumping occur when sea waves are changing the air cushion volume. This results in certain vertical dynamics which can be expressed:

$$\dot{V}_0(t) = A_c\,\zeta_a\,\omega_0\frac{sin\frac{\kappa\,L}{2}}{\frac{\kappa\,L}{2}}cos(\omega_0 t), \tag{10}$$

where we assume zero craft surge speed.

2.1 State Space System

The LTI, system given in eq. (1) – (10), can be written in standard state space form:

$$\dot{x}(t) = A\,x(t)+B\,u(t)+E\,v(t) \tag{11}$$

where:

$$\begin{gathered} x = \left[\,\eta_3\;\;\eta_5\;\;\dot{\eta}_3\;\;\dot{\eta}_5\;\;\mu_u\,\right]^T_{,}\quad u = \Delta A_L,\quad v = \left[\,F_3^e\;\;F_5^e\;\;\dot{V}_0\,\right]^T_{,}\\ A\in\mathbb{R}^{5\times5}_{,}\quad B\in\mathbb{R}^{5\times1}_{,},\quad E\in\mathbb{R}^{3\times5}_{,} \end{gathered} \tag{12}$$

The measurement signal y is a bandpass filtered numerical integration of an accelerometer located at the bow tip. Using the defined coordinate system, Auestad et al. (2013b) shows that this signal can be written:

$$y(t) = Cx(t) = \dot{\eta}_3 - L_b\dot{\eta}_5, \tag{13}$$

where L_b is the longitudinal length to the bow tip (see fig. 3) from our coordinate origin. Also, $C\in\mathbb{R}^{1\times5}$. All coefficients in the system matrices A, B, C and E have physical meanings and are given in App. A.

2.2 Control System Design

The following singel-input-singel-output, motion compensating, proportional feedback control law is proposed:

$$u(t) = -k\,y(t), \tag{14}$$

where $k > 0$ is the controller gain and k, u and $y\in\mathbb{R}$

3. STABILITY ANALYSIS

By combining (11) - (14) and setting $v = 0$, then the unperturbed closed loop system can be written:

$$\begin{aligned} \dot{x} &= (A-BkC)x\\ &= A_{cl}\,x, \end{aligned} \tag{15}$$

Lemma 1. A_{cl} is hurwitz

Proof: The closed loop system matrix is written:

$$A_{cl} = \begin{bmatrix} 0 & 0 & 1 & 0 & 0\\ 0 & 0 & 0 & 1 & 0\\ -\frac{C_{33}}{A_{33}+m} & 0 & -\frac{B_{33}}{A_{33}+m} & 0 & \frac{A_c P_0}{A_{33}+m}\\ 0 & -\frac{C_{55}}{A_{55}+I_{55}} & 0 & -\frac{B_{55}}{A_{55}+I_{55}} & -\frac{A_c P_0 x_{cp}}{A_{55}+I_{55}}\\ 0 & 0 & \alpha & \beta & -\frac{K_3}{K_1} \end{bmatrix},$$

where $\alpha = -\frac{A_c\rho_{c0}+K_2 k}{K_1}$ and $\beta = \frac{A_c\rho_{c0}x_{cp}+\frac{1}{2}K_2 L_b k}{K_1}$.

Choosing the Lyapunov candidate $V(x)$:

$$V(x) = x^T P x \tag{16}$$

The derivative along the system trajectories of the closed loop system yields:

$$\begin{aligned}\dot{V}(x) &= \dot{x}^T P x + x^T P \dot{x} \\ &= x^T (A_{cl}^T P + P A_{cl}) x \\ &:= -x^T Q x\end{aligned} \tag{17}$$

The Lyapunov equation is defined:

$$P A_{cl}^T + A_{cl} P = -Q \tag{18}$$

For A_{cl} to be Hurwitz, and therefore the equilibrium point $x = 0$ to be globally asymptotic stable (GAS), (18) must be fulfilled and there must exist a P, Q s.t. $P > 0$ and $Q \geq 0$. Since the system is linear we can extend our results and claim global exponential stability (GES) of the origin. Due to the structure of A_{cl} and P, the top left $(2{\times}2)$ corner of Q is forced to zero. Therefore, the invariance principle will be used which will prove that a $Q \geq 0$ results in GAS for the closed loop system defined in (15).

Let $P = diag(p_{ii})$, $Q = diag(q_{ii})$ for $i = 1, 2, ..., 5$.

We choose:

$$p_{11} = p_{33} \frac{C_{33}}{A_{33} + m}, \quad p_{22} = p_{44} \frac{C_{55}}{A_{55} + I_{55}}, \quad p_{55} = 1,$$

$$p_{33} = \frac{(A_{33} + m)(A_c \rho_{c0} + K_2 k)}{A_c K_1 P_0}, \, p_{44} = \frac{K_2 L_b k + A_c \rho_{c0} x_{cp}}{A_c K_1 P_0 x_{cp}} \tag{19}$$

As the top left 2×2 submatrix of A_{cl} is zero, the same will hold for the chosen Q hence $q_{11} = q_{22} = 0$. Then choose:

$$q_{33} = \frac{2\, p_{33}\, B_{33}}{(A_{33} + m)}, \quad q_{44} = 2\, p_{44}\, A_c \rho_{c0} x_{cp}, \quad q_{55} = 2\, p_{55} \frac{K_3}{K_1} \tag{20}$$

It can be seen that the solution for P and Q solves the Lyapunov equation (18). Also, $P > 0$ and $Q \geq 0$ since P and Q are diagonal and all the terms in (19) and (20) are positive due to their physical interpretation.

Using the invariant set theorem we can show GES for the equilibrium $x = x_0$. From (15) and (17) it can be seen that:

$$\begin{aligned}\dot{V}(x) &= 0 \\ &\Downarrow \\ x = x_0 &= [\, \eta_3 \;\; \eta_5 \;\; 0 \;\; 0 \;\; 0 \,]^T\end{aligned} \tag{21}$$

However, using the left hand side of (15):

$$\ddot{\eta}_3 = \ddot{\eta}_5 = \dot{\mu}_u = 0, \tag{22}$$

only if

$$\eta_3 = \eta_5 = 0 \tag{23}$$

Hence the equilibrium $x = 0$ is GES for all parametric uncertainties in A, B and C and the result of Lemma 1 follows.

Remark 1. By combining eq. (11) - (14), the perturbed, closed loop system can be written:

$$\dot{x}(t) = A_{cl} x(t) + E v(t) \tag{24}$$

The solution for the perturbed system (24) is uniformly, ultimately bounded by a term b. Hence, $\|x(t)\| \; \leq b \, \forall x$ according to *Lemma* 9.2 in Khalil (2002).

In addition, by using the results from Lemma 1 and by extending our Lyapunov function, with the perturbed term $(v(t) \neq 0)$, it can be seen that:

$$\dot{V} = -x^T Q x + 2 x^T P E v < 0, \tag{25}$$

if we restrict the disturbance vector v to satisfy the inequality:

$$||v(t)|| < ||T\, x(t)||, \tag{26}$$

where $T = \begin{bmatrix} 0 & 0 & B_{33} & 0 & 0 \\ 0 & 0 & 0 & B_{55} & 0 \\ 0 & 0 & 0 & 0 & \frac{K_3}{\rho_{c0}} \end{bmatrix}$, and the vector norm $|| \bullet ||$ denotes the 1-norm (App. A in Khalil (2002)).

4. MODEL TEST RESULTS

4.1 Setup and Notation

In this section, the experimental setup is described.

- The Main Dimensions for the UM Wave Craft are listed in app. B. The model scale factor is 8.
- All tests are performed either at Marine Cybernetics Laboratory (NTNU) or The Towing Tank, both located at SINTEF, Marintek in Trondheim, Norway.
- The craft includes fully scalable SES equipment such as the Ventilation Valve, Lift Fans, Bag Fan, Stern and Aft seal/Bag.
- The input for the control system is an accelerometer (ICSensors, Model 2041) located midships at the bow tip. A SES experience vibrations in the hull, i.e. process disturbances due to the air cushion dynamics. Auestad et al. (2013a) presents proper handling of the raw accelerometer signal.

Experimental model test results will be shown for regular and irregular seas with the MCS toggled OFF/ON.

The following notations will be used:

- 180° sea: Wave direction from the aft.
- MCS OFF: Constant air cushion leakage, $A_L = A_{L,Bias}$
- MCS ON: The proposed controller varies the cushion leakage, $A_L(t) = A_{L,Bias} + \Delta A_L(t)$
- H_s, T_s denotes wave height $[m]$ and period $[s]$. Definitions of H_s involves:
  - · For regular waves: Peak to peak height
  - · For irregular waves: Mean height of the third highest waves
- Motion Damping $:= 100 \left(1 - \frac{\text{Peak to Peak, MCS ON}}{\text{Peak to Peak, MCS OFF}}\right)$
- Bow Pos.: The translation of the bow tip along the Down axis in the North-East-Down frame. These measurements are given by lab equipment (Qualisys, Oqus Camera Series). Mathematically this can be expressed:

$$BowPos. = cos(\eta_4) cos(\eta_5) \int y dt \tag{27}$$

  using Fossen (2011).

4.2 Performance in Regular Waves

In this experiment, the SES encounters regular head sea waves with the MCS toggled OFF and ON. Figure 4 and

5 clearly illustrate the effect of the MCS which is toggled ON at $t = 17s$ and $t = 150s$, respectively.

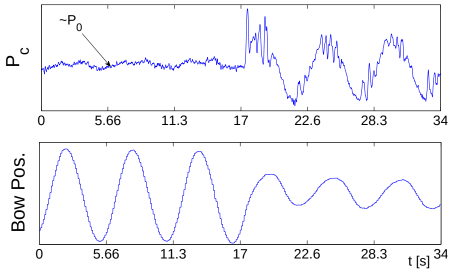

Fig. 4. Head Sea, $H_s = 1.2m$, $T_s = 5.6s$. MCS OFF / ON at $t = 17s$, 68 % Motion Damping

Figure 5 shows the performance of the control system in large long crested waves.

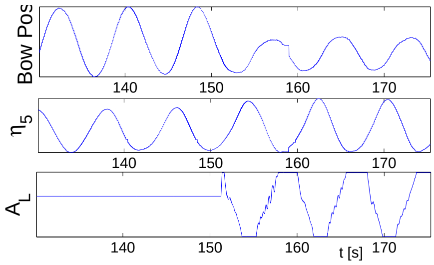

Fig. 5. 135° Sea, $H_s = 2.7m$, $T_s = 8s$. MCS OFF / ON at $t = 151s$, 60 % Motion Damping

4.3 Performance in Irregular Waves

The following model test results illustrates the Power Spectral Density (PSD) for the Bow Pos., see eq. (27).

The duration of each test is approximately an hour with one half MCS ON and one half MCS OFF. The wave spectrum is Jonswap (Fossen, 2011) with $\gamma = 3.3$, $(\sigma_{low}, \sigma_{high}) = (0.007, 0.009)$.

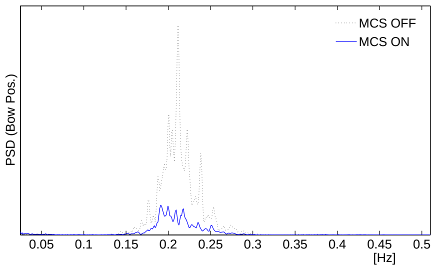

Fig. 6. Head sea, $H_s = 1m$, $T_s = 5s$

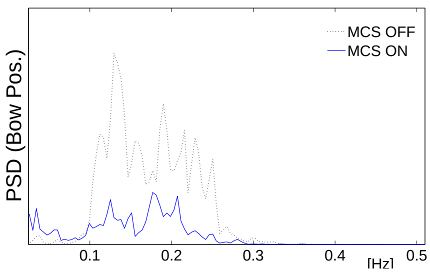

Fig. 11. 135° sea, $H_s = 2m$, $T_s = 7.5s$

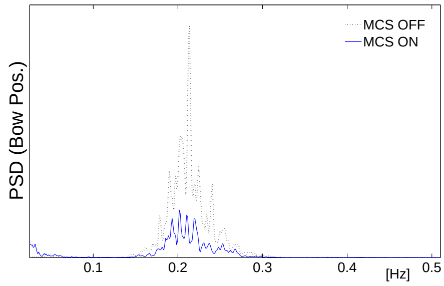

Fig. 7. 45° sea, $H_s = 1m$, $T_s = 5s$

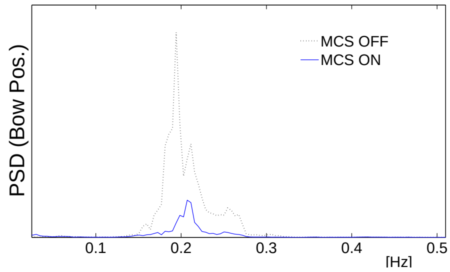

Fig. 8. 135° sea, $H_s = 1m$, $T_s = 5s$

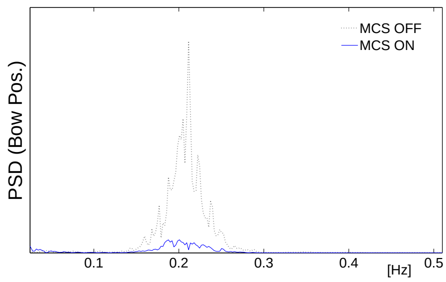

Fig. 9. 180° sea, $H_s = 1m$, $T_s = 5s$

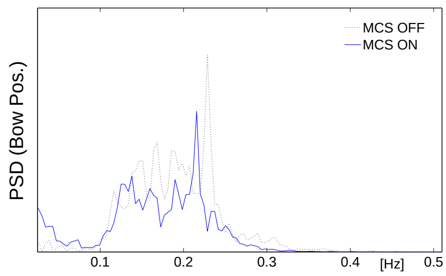

Fig. 10. 90° sea, $H_s = 1.5m$, $T_s = 7s$

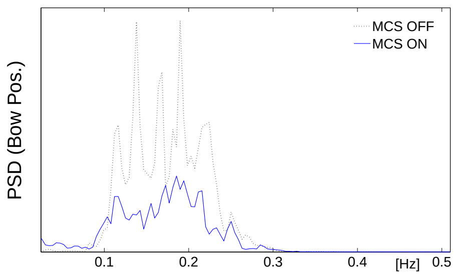

Fig. 12. 45° sea, $H_s = 2.5m$, $T_s = 8s$

The MCS performs best in following seas. A reason for this could be the longitudinal difference in buoyancy. The stern hull has higher buoyancy than the fore part of the hull. For instance, let two sea waves hit the rigid vessel at different time instances, one head sea wave and one following sea wave. Now, it would be reasonable to assume that it is easier to compensate for the vertical position of the bow tip when the wave energy lays on the stern part of the hull instead of on the fore part.

The Power Spectral Density (PSD) plots (fig. 6 - 12) illustrate that the bow tip motions are reduced when the MCS is toggled ON. This is evidently true for all sea wave headings except 90 degree seas, where, as expected, the MCS has small effects since the roll motion are dominating the heave motion in the specific wave period.

Using Kaplan et al. (1981) the uniform pressure resonance is calculated to approximately 1.5 Hz. However, the resonance frequency is not scalable through model testing (Kaplan et al., 1981) and the main reason behind this is the lack of scaling opportunities for P_a. The model test pressure resonance was found to be approximately 10 [Hz], which would correspond to a 3.5 Hz resonance in the full scale domain. However, these high frequencies are not excited at zero surge speed.

5. CONCLUSIONS AND FURTHER WORK

A control system for controlling the vertical position of a Surface Effect Ship at zero vessel speed is presented. The system is named Motion Compensation System (MCS). The stability analysis shows that the non-perturbed, closed loop system is Globally Exponential Stable. The poles of the perturbed closed loop system has strictly negative real values (this proves stable behaviour for any parametric uncertainties using the proposed controller).

The performance of the MCS is illustrated through experimental model testing of a 3 meter long Surface Effect Ship. The performance is presented through time series (figure 4 and 5) and power spectrum density plots (fig. 6 and 12) for regular and irregular seas, respectively. The plots illustrate how the controlled air cushion pressure affects the bow tip motion.

For instance, fig. (6) and (12) illustrate two different waves with two different motion damping ratios, respectively 68% and 60%. This paper successfully illustrates damping of vertical motions of a free floating SES, at zero craft speed, which has not been documented before.

The MCS is not limited to transfer of personnel from a vessel to a wind turbine, it is relevant for every scenario where one wants to control and damp vertical motion at seas. The control point location, which in this case was the bow tip, can easily be changed, even online.

Further work involves work using hybrid control tools when switching between the different phases as explained in section 1.2.

ACKNOWLEDGEMENTS

This work was partly supported by Umoe Mandal and The Research Council of Norway through the Centres of Excellence funding scheme, project number 223254 - AMOS and the Industrial Ph.D. scheme. The model tests were financed by Carbon Trust's Offshore Wind Accelerator program (OWA, 2010)

REFERENCES

Auestad, Ø., Gravdahl, J.T., and Fossen, T.I. (2013a). Heave motion estimation on a craft using a strapdown inertial measurement unit. *The 9th IFAC Conference on Control Applications in Marine Systems (CAMS), Osaka, Japan, 17-20, Sep.*

Auestad, Ø., Gravdahl, J.T., Sørensen, A.J., and Espeland, T.H. (2013b). Simulator and control system design for a free floating surface effect ship at zero vessel speed. *The 2013 IFAC Intelligent Autonomous Vehicles Symposium, Gold Coast, Australia, 26 - 28 June.*

Basturk, H.I. and Krstic, M. (2013). Adaptive wave cancelation by acceleration feedback for ramp-connected air cushion-actuated surface effect ships. *Automatica*, 49(9), 2591–2602.

Butler, E.A. (1985). The surface effect ship. *Naval Engineers Journal*, 97(2), 200–258.

Doctors, L. (2012). Near-field hydrodynamics of a surface-effect ship. *Journal Of Ship Research*, 56(3), 183–196.

EWEA (2013). Deep water - the next step for offshore wind energy. Technical report, European Wind Enery Association, July.

Fossen, T.I. (2011). *Handbook of Marine Craft Hydrodynamics and Motion Control*. John Wiley & Sons, Ltd, UK.

Kaplan, P. and Davies, S. (1974). *A Simplified Representation of the Vertical Plane Dynamics of SES Craft.* AIAA/SNAME Advanced Marine Vehicle Conference.

Kaplan, P.B., Bentson, and Davis, S. (1981). *Dynamics and Hydrodynamics of Surface Effect Ships.* Trans. SNAME VOL 89 1981 page 211 - 247.

Khalil, H.K. (2002). *Nonlinear Systems.* Prentice Hall.

Musial, W. and Ram, B. (2010). *Large-Scale Offshore Wind Power in the United States, p. 116-117.* National Renewable Energy Laboratory.

OWA (2010). Offshore wind accelerator (owa) access competition competition overview and technical specification. *Carbon Trust.*

Sørensen, A.J. (1993). *Modelling and Control of SES Dynamics in the Vertical Plane.* Ph.D. thesis, Department of Engineering Cybernetics, NTNU (Formerly NTH).

Sørensen, A.J. and Egeland, O. (1995). Design of ride control system for surface effect ships using dissipative control. *Automatica*, 31, 183 – 199.

Appendix A. SYMBOLIC MODEL MATRICES

$$A = \begin{bmatrix} 0 & 0 & 1 & 0 & 0 \\ 0 & 0 & 0 & 1 & 0 \\ \frac{-C_{33}}{m+A_{33}} & 0 & \frac{-B_{33}}{m+A_{33}} & 0 & \frac{A_c P_0}{m+A_{33}} \\ 0 & \frac{-C_{55}}{I_{55}+A_{55}} & 0 & \frac{-B_{55}}{I_{55}+A_{55}} & \frac{-A_c\,P_0\,x_{cp}}{I_{55}+A_{55}} \\ 0 & 0 & \frac{-\rho_{c0} A_c}{K_1} & \frac{\rho_{c0}\,A_c\,x_{cp}}{K_1} & \frac{-K_3}{K_1} \end{bmatrix}$$

$$B = \begin{bmatrix} 0 \; 0 \; 0 \; 0 \; \frac{K_2}{K_1} \end{bmatrix}^T \qquad C = [0 \;\, 0 \;\, 1 \;\, -L_b \;\, 0]$$

Appendix B. MAIN DIMENSIONS

Length/Width over all: 26.6/10.4 m, Draught OFF/ON Cushion: 2.77/0.8 m, Passengers: 12 PAX.